International Journal of Thermophysics, Vol. 24, No. 1, January 2003 (© 2003)

Thermophysical Characterization of Elastic Solids: A Novel Application for the Material Testing Machine

M. G. Beghi[1,2] **and L. Luzzi**[3]

Received April 11, 2002

The conventional machine for the mechanical testing of materials finds a new application in thermophysical characterization of a large class of elastic solids, including metals and ceramics. A measuring technique, which is based on the thermoelastic effect and exploits a simple accessory for the testing machine, has been improved and is critically reviewed here. The technique allows the simultaneous measurement of the thermal conductivity and thermal diffusivity, the thermal expansion coefficient or alternatively the specific heat, and the Grüneisen parameter. Operational criteria for measurement and data analysis are presented and discussed. The method has been validated at room temperature using several Certified Reference Materials; its precision and accuracy turn out to be comparable to those of established methods.

KEY WORDS: Certified Reference Materials; Grüneisen parameter; specific heat; thermal conductivity; thermal contact resistance; thermal diffusivity, thermal expansion coefficient; thermo-elasticity.

1. INTRODUCTION

The material testing machine is a well known and widespread piece of equipment which finds an increasing spectrum of applications in the field of materials research and technology. These applications follow the ever increasing spectrum of materials, and of properties useful for their characterization. A further versatile accessory has been developed and patented for this kind of machine, which allows a simultaneous multi-property

[1] Department of Nuclear Engineering, INFM-Politecnico di Milano, via Ponzio 34/3, I-20133 Milano, Italy.

[2] To whom correspondence should be addressed. E-mail: marco.beghi@polimi.it

[3] Department of Nuclear Engineering, Politecnico di Milano, via Ponzio 34/3, I-20133 Milano, Italy.

0195-928X/03/0100-0287/0 © 2003 Plenum Publishing Corporation

thermophysical characterization of elastic solids [1–4]. It is a simple and inexpensive accessory which provides a thermally controlled environment and an accurate temperature measurement system to an otherwise conventional compression test. Earlier versions of the measurement method have been applied to both metallic [1, 2] and ceramic [5] materials. Further developments of the technique are critically reviewed here. Operational guidelines are discussed, and an overall assessment of the method is provided.

2. THEORY

The method is based on the thermoelastic effect, by which elastic deformations of a specimen are associated with an effective heat source active within the specimen itself [2, 6–8]. Cylindrical compression specimens are subjected to a two-stage measurement cycle: a uniaxial loading stage, which activates the heat source, bringing the specimen out of thermal equilibrium, and a thermal relaxation stage at constant stress σ_{rel} (see Fig. 1). The measurement equipment achieves with very good approximation stress and strain fields which are uniaxial and spatially homogeneous throughout the specimen. It also achieves a controlled background temperature field (minimized drift and gradients) and the following controlled thermal boundary conditions: adiabatic lateral surface, constant temperature T_0 of the metallic bearing blocks in contact with specimen bases [1, 2],

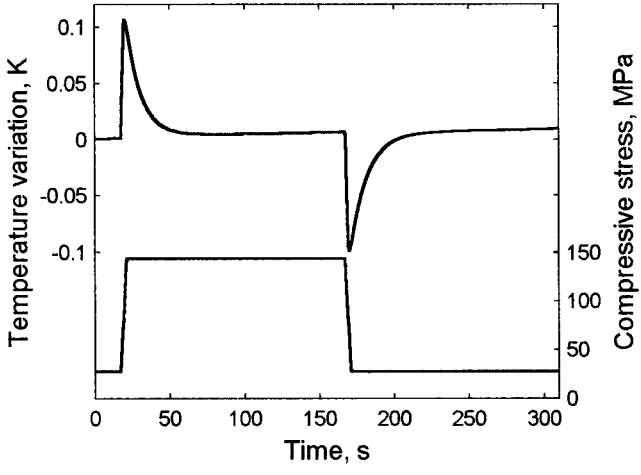

Fig. 1. Compressive stress (lower curve) and temperature variation at specimen mid-plane (upper curve) during a loading-relaxation and an unloading-relaxation cycle.

and a thermal contact resistance R_c [9] being, at most, present between the specimen and bearing blocks.

Under these conditions the temperature field T depends on the axial coordinate x only and the small temperature variations $\theta \equiv T - T_0$ around the equilibrium temperature T_0 are governed by the Fourier equation of the form [2, 3]:

$$\frac{\partial \theta}{\partial t} = \chi \frac{\partial^2 \theta}{\partial x^2} + \frac{\alpha}{\rho c} T_0 \frac{d\sigma}{dt}, \tag{1}$$

where χ is the thermal diffusivity, α is the linear thermal expansion coefficient, ρ is the mass density, c is the specific heat, and σ is the axial stress, taken positive when compressive. Thermal contact resistance (TCR) boundary conditions,

$$\frac{\theta(\pm H/2, t)}{R_c} = \mp \lambda \left. \frac{\partial \theta}{\partial x} \right|_{x = \pm H/2}, \tag{2}$$

are considered, where λ is the thermal conductivity and H is the specimen height. Starting from the thermal equilibrium condition $\theta(x, t = 0) = 0$, the loading stage is conducted at constant stress rate $d\sigma/dt$ for a time t_0. Equations (1) and (2) are integrated by series expansion [3, 10]; in the relaxation stage, all the higher-order terms decay significantly faster, and after a short transient, the temperature field is well represented by the leading order term. At the specimen mid-plane ($x = 0$), this term is

$$\theta(0, t) \cong \theta_{\max} \exp[-(t - t_0)/\tau_0] \qquad (t - t_0) > \tau_0, \tag{3}$$

where the time constant τ_0 and the temperature amplitude $\theta_{\max}$ are given by

$$\tau_0 = H^2/(4\chi\beta_0^2) \tag{4}$$

and

$$\theta_{\max} = \left(\frac{\alpha}{\rho c}\right) \frac{F}{G(\beta_0)}. \tag{5}$$

The two parameters F and $G(\beta_0)$ are defined as

$$F \equiv \frac{d\sigma}{dt} T_0 \tau_0 [1 - \exp(-t_0/\tau_0)] \tag{6}$$

and

$$G(\beta_0) \equiv \left(\frac{\beta_0}{2 \sin \beta_0} + \frac{\cos \beta_0}{2} \right). \tag{7}$$

The nondimensional numerical value β_0 is the solution, in the interval $(0, \pi/2)$, of the transcendental equation

$$\beta_0 \tan \beta_0 = \frac{H}{2\lambda R_c} \equiv \frac{1}{r}, \tag{8}$$

whose right-hand side has a useful interpretation. The thermal resistance (per unit cross-sectional area) between the specimen mid-plane and the bearing blocks in contact with its bases is the series of the conductive resistance $R_\lambda = H/(2\lambda)$ and the contact resistance R_c; the ratio $r \equiv R_c/R_\lambda$ gives the relative importance of R_c. For the measurement of transport properties of the material, i.e., λ and χ, R_c represents a spurious effect, which is particularly relevant for short and/or highly conductive specimens—see Eq. (8).

The temperature variation measured at the mid-plane during the last segment of the thermal relaxation, which is typically of the order of 0.1 K, can be fitted to the form in Eq. (3), obtaining τ_0 and $\theta_{\max}$. A procedure, based on the same type of measurement performed on reference specimens of independently known properties, was devised to calibrate the contact resistance. The procedure, described in detail in Ref. 3, gives a calibration curve $R_c^*(\sigma_{\text{rel}})$; exploiting this curve (TCR case), a two-fold possibility opens for data analysis. The first possibility assumes the heat capacity per unit volume ρc is independently known; Eq. (8) is then cast in the form

$$\frac{\tan \beta_0}{\beta_0} = \frac{\tau_0}{(H/2)\, R_c^* \rho c}, \tag{9}$$

from which β_0 is numerically determined, and the thermal expansion coefficient α is given by Eq. (5). The second possibility assumes instead that the thermal expansion coefficient α is independently known; in this case, β_0 is the solution, in the interval $(0, \pi/2)$, of the transcendental equation

$$\frac{\tan \beta_0}{\beta_0} G(\beta_0) = \frac{1}{F} \frac{\tau_0 \theta_{\max}}{(H/2)\, R_c^* \alpha}, \tag{10}$$

and ρc is given by Eq. (5). In both cases Eq. (4) gives directly the thermal diffusivity χ and conductivity $\lambda = \chi \rho c$. If the elastic properties of the

specimen are also known (Young's modulus E and Poisson's ratio ν), the Grüneisen parameter $\gamma = (\alpha/(\rho c))\, E/(1-2\nu)$ can also be obtained.

It is worth noting that in the limit $R_c \to 0$ the boundary conditions, Eq. (2), become the isothermal conditions (ISO case): $\theta(\pm H/2, t) = 0$; in this case, $r \to 0$, $\beta_0 \to \pi/2$ and the diffusivity is given, directly and independently from other results, by [1]

$$\chi = H^2/(\tau_0 \pi^2). \tag{11}$$

3. EXPERIMENT

A conventional material testing machine is used, which must be operated in compression under load control and at constant stress rate. The accessory is described elsewhere in detail [1–3]; it consists of spherically seated compression platens, molybdenum bearing blocks, a thermal conditioning system, and an appropriate temperature sensor. The measurement requires recording of two signals: the temperature at the specimen midplane and the applied load (see Fig. 1).

Cylindrical specimens (typically of millimeters to centimeters scale) are adopted, similar to the standard ones for compression tests [11, 12]; in order to achieve an accurate thermophysical characterization, they must satisfy some requirements about dimensions (optimal ranges for height H and diameter D) and finishing (bases plane and parallel to a close tolerance, and lap-finished). The specimen height H determines the thermal relaxation constant τ_0; an *a priori* estimation of τ_0 can be obtained by Eq. (11) and an approximate guess for the value of χ, and is useful to set experimental parameters (see below). The specimen diameter D determines the load level, and, therefore, the required capacity of the testing machine. Ratios H/D in the range 3 to 8 have been found to be appropriate for transversal uniformity of both stress and temperature [1, 2].

The temperature signals to be measured have small amplitude (typically 0.03 to 0.1 K) and relatively limited duration (typically of the order of tens of seconds); their accurate measurement requires sensors of sufficient sensitivity and response time. Accurate calibration is crucial, since the obtained values of $\alpha/(\rho c)$ and γ are directly proportional to the measured temperature variation—see Eq. (5). The measurements presented in this study were performed by thermistors, which offer a good combination of the mentioned requisites, and for which an individual calibration procedure has been developed [2]. The time response of the measurement system can be represented with sufficient accuracy by a single-pole transfer function, characterized by a time constant τ_s. The value of τ_s can be derived from the load and temperature recorded during the experiment [2].

The specimen mounting procedure is the standard one for compression tests [11, 12]; between the specimen and the bearing blocks, a lubricant [13] is interposed as well as a thin film of a conductive filler [9, 14, 15], which aims at minimizing and controlling the thermal contact resistance R_c. For accurate measurement of the thermal diffusivity, namely of short and/or highly conductive specimens, a preliminary calibration of contact resistance is required; this is accomplished by a simple procedure which supplies a calibration curve $R_c^*(\sigma_{\rm rel})$ for the contact resistance and its dependence on the contact pressure $\sigma_{\rm rel}$ at which relaxation occurs [3].

For each measurement cycle the following operational parameters have to be appropriately selected: stress variation $\Delta\sigma$, duration t_0 of the loading stage, and relaxation stress $\sigma_{\rm rel}$. Stress variation $\Delta\sigma$ must be large enough to produce a sufficient temperature variation (typically a few tens of MPa). The relaxation stress $\sigma_{\rm rel}$ must be smaller than the yield stress for the material, and fall in a range for which a calibration curve $R_c^*(\sigma_{\rm rel})$ applicable to a wide range of materials can be found (the 50 to 100 MPa interval has proven to be appropriate) [3]. The loading stage duration t_0 must satisfy the conditions $\tau_0 > t_0 > \tau_s$; it must be long enough to avoid serious signal distortion by limited sensor response, and short enough to avoid signal reduction by thermal conduction. Relaxation distortion by limited sensor response is avoided if the condition $\tau_0 > 10\tau_s$ is satisfied, which sets a lower limit on the specimen height H—see Eq. (11). Time constants τ_s of about 0.3 s are typically achieved [2], which set a lower limit of ~ 3 s on τ_0, meaning minimum values of H ranging from millimeters to a few centimeters. On the other hand, excessive values of H, and therefore of τ_0, are unfavorable as they lead to longer test duration, i.e., higher sensitivity to temperature drifts [1, 2]. The transient is exhausted in $\sim 5\tau_0$, and an appropriate total recording time is $\sim 15\tau_0$.

Figure 2 shows that the recorded temperature relaxation eventually becomes exponential—see Eq. (3); the time constant τ_0 and the amplitude $\theta_{\max}$ are obtained by a least-squares regression, after subtraction of a baseline temperature [1, 2]. Figure 2 also shows the theoretical specimen surface temperature, computed by the full solution of Eqs. (1) and (2) exploiting the results of the regression, and its convolution with the thermistor transfer function. The agreement between the computed (including the sensor response) and the measured temperatures confirms that the adopted model correctly represents the physical conditions.

In this work the values of τ_0 and $\theta_{\max}$ are used following the first of the two possibilities indicated in Section 2 for the TCR case—see Eq. (9). The values of $R_c^*(\sigma_{\rm rel})$ are given by the calibration curve

$$R_c^*(\sigma_{\rm rel}) = \frac{dR}{d\sigma}(\sigma_{\rm rel} - \sigma_0) + R_{\sigma_0} \tag{12}$$

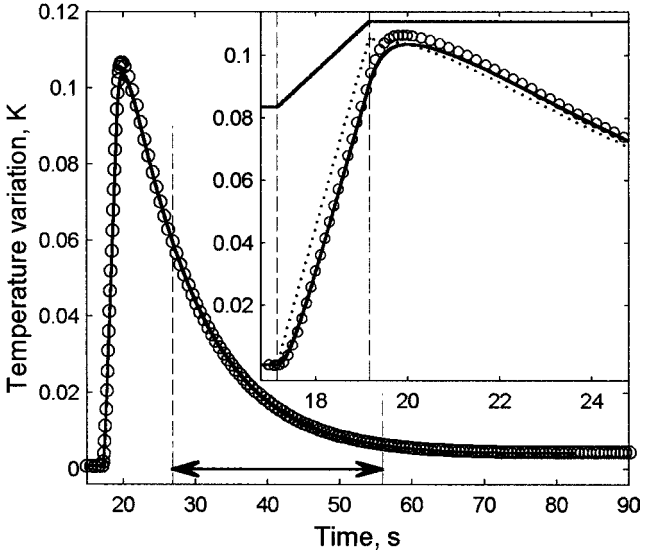

Fig. 2. Loading-relaxation cycle (magnification of Fig. 1). Circles: measured temperature (sampling frequency is reduced for clarity). Continuous line: theoretical specimen temperature [3] computed with the best fit parameters (the regression interval is shown by the arrow), convoluted with a single-pole thermistor transfer function [2]; the thermistor time constant τ_s is obtained from the delay between load and temperature variation [2]. In the inset: further magnification of the loading stage. Upper curve: compressive stress of Fig. 1, with indication of the loading stage duration t_0; circles and continuous line as above; dotted line: theoretical specimen temperature [3] computed with the best fit parameters.

($dR/d\sigma = -7.78 \times 10^{-8}$ m$^2 \cdot$K$\cdot$W$^{-1} \cdot$MPa^{-1}, $R_{\sigma_0} = 1.43 \times 10^{-5}$ m$^2 \cdot$K$\cdot$W^{-1} and $\sigma_0 = 50$ MPa), obtained by the procedure of Ref. 3 on the set of reference specimens of Table I, with $50 < \sigma_{\text{rel}} < 100$ MPa.

4. RESULTS

The equipment was tested on several material testing machines, and the repeatability of results was ascertained [1]. In the present work tests were performed at room temperature using the following experimental setup: an Instron 1121 testing machine of 10 kN capacity operated under load control, a measurement chamber for thermal conditioning [1] made by a 10 mm thick aluminium cylinder, and temperature sensed by a sintered bead microthermistor of the negative temperature coefficient (NTC) type [2]. The appropriate mechanical and thermal conditions at the specimen

Table I. Set of Specimens Adopted as Reference Materials

Material		H	ρ	c_{ref}	χ_{ref}	λ_{ref}	α_{ref}	R_λ
Composition (wt%)	Sample	(mm)	($kg \cdot cm^{-3}$)	($J \cdot kg^{-1} \cdot K^{-1}$)	($10^{-6} m^2 \cdot s^{-1}$)	($W \cdot m^{-1} \cdot K^{-1}$)	($10^{-6} K^{-1}$)	($10^{-5} m^2 \cdot K \cdot W^{-1}$)
Copper 99.90	CU1	49.5	8.933	385	117	398	16.71[a]	6.22
Copper 99.999+	CU2	100	8.933	384.9[a]	117	398	16.5	12.6
Aluminium 99.9	AL	70.0	2.702	903	96.8	237	23.1	14.8
Molybdenum 99.95	MO1	39.5	10.240	249.6[a]	54.3	138	4.8	14.3
	MO2	57.0	10.240	249.6[a]	54.3	138	4.8	20.6
Electrolytic Iron 99.90	FE1	42.0	7.867	447	21.7[b]	76.4[a]	11.8	27.5
	FE2	50.4	7.867	447	21.7[b]	76.4[a]	11.8	33.0
Titanium 99.5	TI	24.4	4.500	522	9.25	21.9	8.6	55.7
Stainless Steel AISI 446	AISI1	14.9	7.599	460[c]	5.41	18.9[b]	9.86[a]	39.4
	AISI2	19.8	7.599	460[c]	5.41	18.9[b]	9.86[a]	52.4
Austenitic Steel 20.2 Ni–16.2 Cr	NICR1	12.5	8.007	502[c]	3.56[b]	14.3[a]	18[d]	43.7
	NICR2	14.6	8.007	502[c]	3.56[b]	14.3[a]	18[d]	51.0

[a] Values certified by NIST [17, 18].
[b] Obtained by relation $\lambda = \chi \rho c$.
[c] measured by differential scanning calorimetry.
[d] measured by thermomechanical analysis.

bases are obtained by bearing blocks (molybdenum disks, 8 mm thick) and the interposition of a lubricant (mixture of stearic acid and nonpolar vaseline) [12] and a conductive filler (silver platelets, 5 μm thick) [3]. The calibration for contact resistance—see Eq. (12)—was performed under identical experimental conditions.

Measurements were performed on the set of specimens presented in Table I (reference values at room temperature). Their dimensions vary within the above specified limits, and they were all ground to have bases plane and parallel to within 0.01 mm, and lap-finished. These specimens were adopted as reference materials; their choice was not trivial because the measurement method presented here is a multi-property method, whose validation would, in principle, require reference materials with simultaneous certified values of several properties [16]. The specimens of Table I were selected in order to assess the measurement accuracy for various properties and for significant ranges of each of them. Most of the specimens are Certified Reference Materials (CRMs) [17, 18] for one of the involved properties, and for the other properties, recommended values [19, 20] are available; the aluminium and titanium specimens are instead high-purity materials, for which recommended values of thermophysical properties are available [19, 20]. Table I also presents the conductive resistance $R_\lambda = H/(2\lambda_{\text{ref}})$ evaluated for each specimen by the reference value of thermal conductivity λ_{ref}.

Table II summarizes the results obtained by the thermoelastic measurements and the TCR data analysis indicated at the end of Section 3, exploiting the reference values ρc_{ref} in order to assess the precision and

Table II. Measured Thermophysical Properties at Room Temperature

Material sample	χ $(10^{-6}\,\text{m}^2\cdot\text{s}^{-1})$	λ $(\text{W}\cdot\text{m}^{-1}\cdot\text{K}^{-1})$	α $(10^{-6}\,\text{K}^{-1})$	γ [-]
CU1	123	423	17.6	2.1
CU2	121	416	17.1	2.1
AL	99.5	243	23.6	2.2
MO1	52.2	133	5.01	1.5
MO2	52.8	135	4.98	1.5
FE1	21.883	76.95	11.6	1.7
FE2	21.881	76.94	11.6	1.7
TI	9.32	21.9	8.43	1.6
AISI1	5.38	18.81	9.57	/
AISI2	5.39	18.84	9.52	/
NICR1	3.536	14.21	17.6	/
NICR2	3.541	14.23	17.5	/

accuracy of the method without involving the uncertainties connected to an auxiliary measurement of the product ρc. The presented values are the averages of results obtained with values of σ_{rel} varying in the 50 to 100 MPa interval; some results are quoted with extra digits to better appreciate small differences. The scatter of results obtained with different values of σ_{rel} is within 2% for χ and λ [3], and within 1% for α [2]; for given values of E and ν [21], the same scatter of 1% is found for the Grüneisen parameter γ. This scatter is completely random and does not correlate with contact pressure σ_{rel}.

5. DISCUSSION

The results can be analyzed in terms of the data in Table III. The first two columns present the uncertainties for χ and α of Table II, obtained by the TCR data analysis, evaluated as $a_v = (v - v_{ref})/v_{ref}$, where v is the average measured value and v_{ref} is the reference value, and $v = \chi$ or $v = \alpha$. Uncertainties are presented only for a transport property (χ) and a thermodynamic property (α), since they are representative of the uncertainties achievable by the thermoelastic method for the transport and, respectively, the thermodynamic properties. For both classes the uncertainty is always within 5%, and in many cases, better than 3%.

For other widespread measurement methods for these same properties [16, 19] systematic comparative assessments of uncertainties are not available in the literature, but indications can be obtained from various sources. From these indications it can be said that uncertainties typically

Table III. Uncertainty of Results with Thermoelastic Measuring Technique

Material sample	$a_{\chi\,(TCR)}$ (%)	$a_{\alpha\,(TCR)}$ (%)	R_c ($10^{-6}\,m^2 \cdot K \cdot W^{-1}$)	r [-]	r^* [-]	$a_{\chi\,(ISO)}$ (%)	$a_{\alpha\,(ISO)}$ (%)
CU1	+5.1	+5.3	9.9	0.160	0.198	−28	+2.8
CU2	+3.4	+3.6	9.5	0.075	0.098	−15	+2.7
AL	+2.8	+2.2	10.5	0.071	0.083	−13	+1.5
MO1	−3.9	+4.4	15.0	0.105	0.086	−19	+3.8
MO2	−2.8	+3.7	14.8	0.072	0.060	−14	+3.3
FE1	+0.8	−1.7	11.3	0.041	0.045	−7.4	−1.6
FE2	+0.8	−1.7	11.1	0.034	0.037	−6.4	−1.7
TI	+0.7	−2.0	12.5	0.022	0.022	−3.4	−1.9
AISI1	−0.5	−2.9	13.2	0.033	0.031	−6.3	−3.1
AISI2	−0.4	−3.4	13.0	0.025	0.023	−4.8	−3.5
NICR1	−0.7	−2.2	13.7	0.031	0.028	−6.2	−2.5
NICR2	−0.5	−2.8	13.6	0.027	0.024	−5.0	−2.8

lie in the 1 to 5% range. The precision and accuracy of the thermoelastic method are therefore comparable to those of established methods.

Table III presents further elements for the assessment of the results of the present study. These include, firstly, the thermal contact resistances R_c measured at 75 MPa for each of the reference specimens following the procedure of Ref. 3, and the corresponding ratios $r = R_c/R_\lambda$; secondly, the ratios $r^* \equiv R_c^*/R_\lambda$ evaluated at 75 MPa by the value R_c^* supplied by the calibration curve (12); and, thirdly, the uncertainties obtained for χ and α by the simpler ISO data analysis [1, 2], which neglects the effect of R_c on thermal relaxation.

The ratio r measures the relative importance of the contact resistance, which explains the various values of $a_{\chi\,(\mathrm{ISO})}$: for $r < 0.025$ the uncertainty $a_{\chi\,(\mathrm{ISO})}$ remains within 5% at most, for $r < 0.05$ it remains within 10%, while for larger values of r, the results become merely qualitative, the thermal diffusivity being always underestimated. Furthermore, with the ISO data analysis the results show a scatter of the order of 5%, correlated to σ_{rel} [1]. The uncertainty $a_{\alpha\,(\mathrm{ISO})}$ is instead not correlated with the r value, and remains within 4%, with the precision being of the order of 1% [2].

The more complete TCR data analysis significantly improves the precision and accuracy of χ, and the dependence on σ_{rel} disappears [3]. $a_{\chi\,(\mathrm{TCR})}$ remains within 5% also at high values of r, being below 3% in most cases; and the precision and accuracy of α, which are already good for the ISO analysis procedure, remain essentially the same for the TCR analysis.

In practice, for an unknown specimen, only the ratio r^* can be estimated, and supplies a criterion to select the data analysis procedure; for $r^* < 0.025$ the ISO procedure, which does not require contact resistance calibration, gives uncertainties within 5% for both χ and α. Short and/or highly conductive specimens lead instead to higher values of r^*; in this case, uncertainties within 5% can still be obtained for both χ and α, but for χ the more complete TCR procedure is required.

6. CONCLUDING REMARKS

It can be concluded that with a simple, inexpensive and easily mounted accessory and with specimens of the same type as those commonly used for compression tests, the material testing machine finds a new interesting application in the thermophysical characterization of elastic solids. The thermoelastic method presented here requires recording of only two signals (load and temperature) in nondestructive tests lasting a few minutes: an independent measurement of either specific heat or thermal expansion coefficient, and in some cases, a calibration of thermal contact resistance. The technique achieves a simultaneous characterization of both transport

and thermodynamic properties, whose precision and accuracy are competitive with those of established methods.

REFERENCES

1. M. G. Beghi and L. Luzzi, *Meas. Sci. and Technol.* **10**:1266 (1999).
2. M. G. Beghi and L. Luzzi, *Rev. Sci. Instrum.* **71**:154 (2000).
3. M. G. Beghi and L. Luzzi, *Meas. Sci. and Technol.* **11**:766 (2000).
4. L. Luzzi and M. G. Beghi, *Device for Measuring Thermophysical Properties of Solid Materials and Method therefor* (Politecnico di Milano, Department of Nuclear Engineering, Milan, 1998) Italian Patent MI98A-0011967 and European Patent Application No 99116677-8.
5. F. Vettraino, G. Magnani, T. La Torretta, E. Marmo, S. Coelli, L. Luzzi, P. Ossi, and G. Zappa, *J. Nucl. Mater.* **274**:23 (1999).
6. D. C. Wallace, *Thermodynamics of Crystals* (John Wiley, New York, 1972), pp. 23–28.
7. M. G. Beghi, C. E. Bottani, and G.Caglioti, *Res Mechanica* **19:** 365 (1986).
8. M. G. Beghi, in *Thermoelastic Stress Analysis*, N. Harwood and W. M. Cummings, eds. (Adam Hilger, Bristol, 1991), pp. 35–43.
9. E. Fried, in *Thermal Conductivity*, R. P. Tye, ed. (Academic Press, New York, 1969), pp. 253–274.
10. H. S. Carslaw and J. C. Jaeger, *Conduction of Heat in Solids* (Clarendon Press, Oxford, 1959), pp. 119–120.
11. ASTM E209, *Standard Practice for Compression Tests of Metallic Materials at Elevated Temperatures with Conventional or Rapid Heating Rates and Strain Rates* (American Society for Testing and Materials, West Conshohocken, PA, 1988).
12. ASTM C39, *Standard Test Method for Compressive Strength of Cylindrical Concrete Specimens* (American Society for Testing and Materials, West Conshohocken, PA, 1996).
13. J. F. Labuz and J. M. Bridell, *Int. J. Rock Mech. Min. Sci. & Geomech. Abstr.* **30**:451 (1993).
14. B. Snaith, P. W. O'Callaghan, and S. D. Probert, *Appl. Energy* **16**:175 (1984).
15. C. V. Madhusudana, *Thermal Contact Conductance* (Springer-Verlag, New York, 1996), pp. 77–99.
16. K. D. Maglíc, A. Cezairlyian, and V. E. Peletsky, eds., *Compendium of Thermophysical Property Measurement Methods* (Plenum, New York, 1984), Vols. 1 and 2.
17. NIST SRM Program, *Certified Reference Materials SRMs 736L1, 738, 5, 781D2* (U.S. Department of Commerce, National Institute of Standards and Technology, Gaithersburg, Maryland).
18. J. G. Hust and A. B. Lankford, *Update of Thermal Conductivity and Electrical Resistivity of Electrolytic Iron, Tungsten and Stainless Steel* (U.S. Government Printing Office, Washington, DC, 1984), NBS Special Publication 260-90.
19. Y. S. Touloukian and C. Y. Ho, eds., *Thermophysical Properties of Matter* (IFI/Plenum, New York), Vols. 2, 10, and 12.
20. F. P. Incropera and D. P. DeWitt, *Fundamentals of Heat and Mass Transfer*, 4th edn. (John Wiley, New York, 1996), pp. 827–831.
21. C. J. Smithells, ed., *Metals Reference Book*, 5th Ed. (Butterworths, London, 1976), pp. 975–976.